International Journal of Applied Engineering Research
ISSN 0973-4562 Volume 10, Number 3 (2015) pp. 7385-7400
© Research India Publications
http://www.ripublication.com

# Block Based Steganalysis With Contourlet And ELM

**[1]T.J.Benedict Jose and [2]Dr. P. Eswaran**

*[1]Research Scholar, Manonmaniam Sundaranar University, Tamilnadu,*
*[2]Department of Computer Science, Alagappa University, Tamilnadu, India.*

**Abstract**

Certain techniques are available to detect whether or not the digital image has something embedded into it. These techniques are steganalysis techniques. In this work, a steganalysis technique is proposed. Initially, the image is decomposed into several blocks by k-means algorithm. After successful clustering of pixels, contourlet is applied over each block of an image. Then, features such as Gray level Non-Uniformity, Run Length Non-Uniformity, Run Percentage and Long Run Emphasis are extracted from the image blocks. Extreme Learning Machine (ELM) is trained with the extracted features. The trained ELM can be tested with different images. The same process of feature extraction is carried out in the testing stage and the final decision of whether or not the image is normal is made by the ELM.

**Keywords**- Steganalysis, contourlet, ELM.

## 1. Introduction

Steganography is the science of embedding sensitive information into a digital image, in order to safeguard the secret message against intruders. The main difference between cryptography and steganography is the way of safeguarding secret messages. Cryptography scrambles the secret message in an unintelligible format, whereas steganography hides the secret information into a cover medium, preferably a digital image. Steganography is least prone to vicious attacks.

A digital image that is proposed to carry a secret image is the cover image. The same digital image is the stego image, after embedding the secret message into it. The hidden secret cannot be visible to human eyes. However, certain techniques are available to detect whether or not the digital image has something embedded into it. These techniques are steganalysis techniques [1, 2].

The steganalysis techniques can be differentiated into two different techniques. They are the steganalysis techniques meant only for certain steganographic techniques and the steganalysis techniques that are widely meant for several steganographic techniques. The techniques which fall on the first type focus on the features of an image that are altered by the embedding algorithm.

The second category of steganalyis techniques work by the principle of extracting features of the cover image that may get altered, during embedding the secret. The extracted features are used for deciding whether the image is normal or a stego image. There are several universal blind steganalysis techniques and they differ from each other by the features being exploited to differentiate between the normal and the stego image.

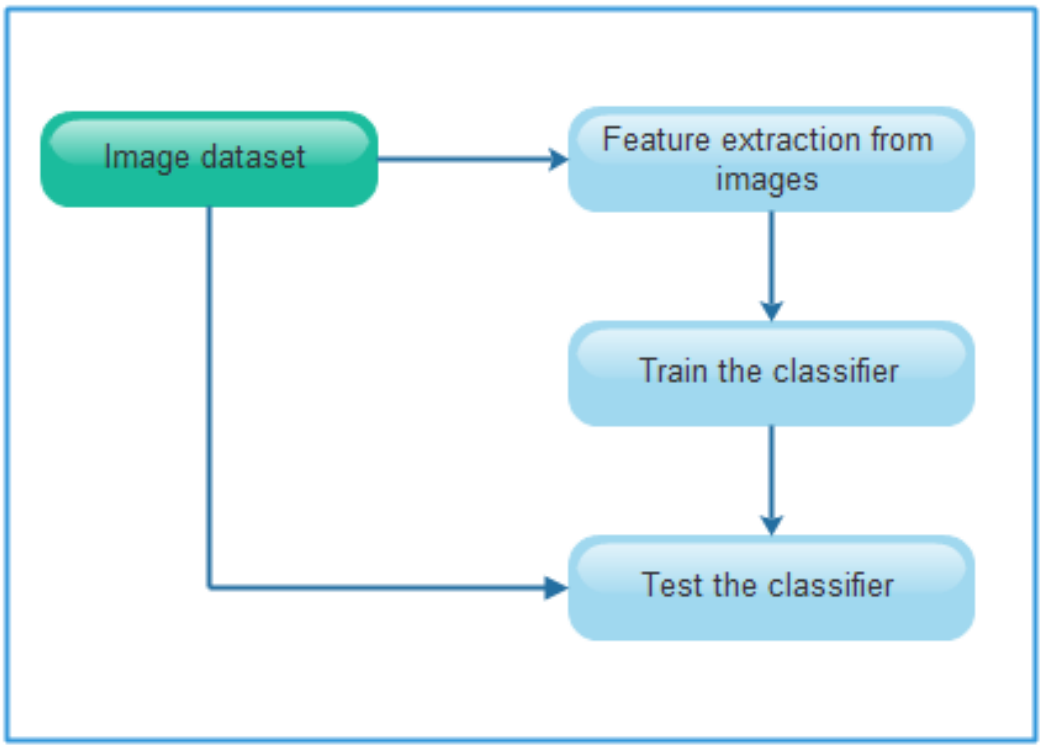


**Fig 1: General structure of a steganalysis scheme**

The common structure of a blind steganalysis technique is to excerpt some features from the images, followed by the utilization of a classifier, the classifier is then given training with the extracted features and finally it can be tested. The common structure is depicted in figure 1.

In this work, the image is decomposed into several blocks by k-means algorithm. After successful clustering of pixels, contourlet is applied over each block of an image. Then, features such as Gray level non-uniformity, Run length non-uniformity, run percentage and long run emphasis are extracted from the image blocks. Extreme Learning Machine (ELM) is trained with the extracted features. The trained ELM can be tested with different images. The same process of feature extraction is carried out in the testing stage and the final decision of whether or not the image is normal is made by the ELM.

## 2. Background

A steganalysis method is presented in [3] by extracting the features of an image. The features are extracted in JPEG domain. Fisher Linear Discriminant is employed as the classifier. The work proposed in [4] distinguishes between the normal and stego images by extracting the features by employing SVM. In [5], a steganalysis technique is proposed in which both the DCT and reduced Markov based features are extracted. SVM is utiized in this work.

A steganalysis scheme is presented on the basis of Subtractive Pixel Adjacency Matrix (SPAM) features and SVM is employed as the classifier [6]. The features with Neighbouring Joint Density probability are extracted in the DCT domain [7] and SVM is used as the classifier.

A Markov chain based steganalysis method is proposed in [8], which calculates the empirical transition matrix is computed and SVM is employed as the classifier. The work presented in [9] exploits feature from gray level run length matrices and the classifier used is SVM.

In [10], a steganalysis method based on the residual value of the pixels is proposed and SVM is employed as the classifier. In [11], a steganalysis algorithm is presented with its root on GLCM and contourlet.

Motivated by the above presented works, this work proposes a steganalytic algorithm that is based on contourlet and several features of an image. ELM is employed as the classifier.

## 3. Proposed Work

This work aims at providing an effective steganalysis algorithm that effectively distinguishes between the normal and the stego images. Initially, an image is decomposed into several blocks and contourlet is applied over images. Then, certain features are extracted from the images and ELM is trained with the extracted features.

This is followed by the testing phase, in which the image is tested by feature extraction. Finally, ELM classifies the image either as normal or stego image. This work involves four stages and they are given below.

1. Decomposing an image into blocks
2. Contourlet application
3. Feature extraction
4. ELM Classification

### 3.1 Decomposing an image into blocks

Initially, the image is split up into several blocks by k-means algorithm. Initially, the number of cluster centers and the number of points are determined. The main advantage of this block based steganalysis is that it follows divide by conquer strategy and thus the results are more accurate.

**Algorithm**

Input: Determine number of cluster centers, array of points;

Step 1: Allocate each pixel to the nearest cluster center
Step 2: Every cluster center has to accomodate pixels
Step 3: Fix each cluster center to the average of the allotted pixels.
Step 4: Repeat steps 1 to 3 until all the pixels are converged
End;

Thus, the above simple k-means algorithm groups the pixels into several clusters or blocks. These blocks are processed further. The main advantage of computing blocks is its simplicity of processing. As all the further operations are applied over these blocks, the results are more accurate than when images are treated as a whole.

### 3.2 Contourlet Transform Application

The contourlet transform consists of two major stages: the subband decomposition and the directional transform. At the first stage, Laplacian pyramid( LP) is used to decompose the image into subbands, and then the second one is a Directional Filter Bank(DFB) which is used to analyze each detail image[11, 12].

#### 3.2.1 Multiresolution Analysis

In the followings and for simplicity, the case with orthogonal filters, which lead to tight frames will be considered only. Multiresolution analysis is divided into the following two analysis:

#### 3.2.2 Multiscale Analysis

This is the multiresolution analysis for the LP, which is similar to the one for wavelets. Suppose that the LP in the contourlet filter bank uses orthogonal filters and down sampling by 2 in each dimension as shown in Fig.(1), which is given as in eqn (1).

$$M = diag(2,2) \tag{1}$$

Under certain regularity conditions, the lowpass synthesis filter *G* in the iterated LP uniquely defines a unique scaling function $\varphi(t)\epsilon L_2 R^2$ that satisfies the following two-scale equation [13]:

$$\sqrt{2}\,\varphi(t) = 2\sum_{n\in Z^2} g[n]\varphi(2t-n) \tag{2}$$

where g[n] is the impulse response of the lowpass synthesis filter G.

$$\text{Let } {}_{j,n} = 2^{-j}\varphi\left(\frac{t-2^j n}{2^j}\right),\ \text{j}\in Z, n \in Z^2 \tag{3}$$

Then the family $\{\varphi_{j,n}\}n \in Z^2$ Is an orthonormal basis for an approximation subspace Vj at the scale $2^j$. Furthermore, provides a sequence of multiresolution nested subspaces $....V_2 \Subset V_1 \Subset V_0 \Subset V_{-1} \Subset V_{-2}...$, where Vj is associated with a

uniform grid of intervals 2j 2j that characterizes image approximation at scale 2j.

The difference images in the LP contain the details necessary to increase the resolution between two consecutive approximation subspaces. Therefore, the difference images live in a subspace Wj that is the orthogonal complement of Vj in Vj-1,as shown in Fig.(2.a), or

$$V_{j-1=}V_j \oplus W_j \tag{4}$$

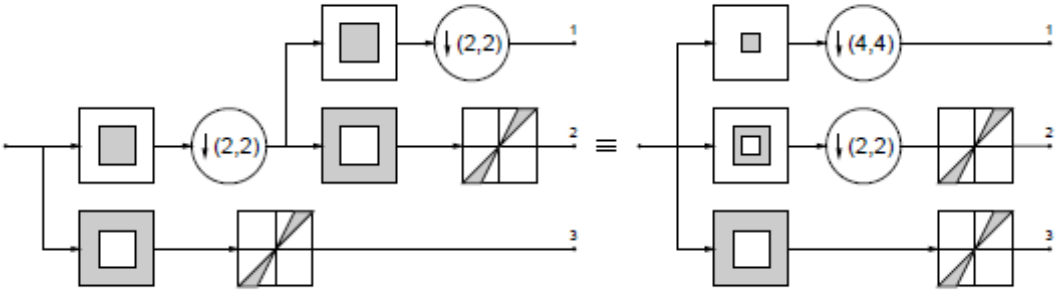


**Fig 2: Contourlet Transform with 2 levels of multiscale decomposition**

It is believed that the LP can be considered as an oversampled filter bank where each polyphase component of the difference image d[n] in Fig(1), together with the coarse image c[n],comes from a separate filter bank channel with the same sampling matrix M = diag (2,2).

Let Fi (z), 0 ≤i ≤ 3 be the synthesis filters for these polyphase components. These are highpass filters. As for wavelets, a continuous function $\Psi^{(i)}(t)$, can be associated with each of these filters, where

$$\sqrt{2}\,\Psi^{(i)}(t) = 2\sum_{n\in Z^2} f_1[n](2t-n) \tag{5}$$

where fi[n] is the impulse response of the highpass synthesis filter Fi(z). So, letting $\Psi^{(i)}(t)$ in (4) be in the form

$$\Psi_{j,n}^{(i)}(t) = 2^{-j}\Psi^{(t)}\left(\frac{t-2^j n}{2^j}\right), j \in Z, n \in Z^2 \tag{6}$$

Then, for scale $2_j$ , $\left\{\Psi_{j,n}^{(i)}\right\}$ 0≤i≤3,n∈ $Z^2$ is tight frame for *Wj*. For all scales, $\left\{\Psi_{j,n}^{(i)}\right\}$ j∈ $Z^2$ 0≤i≤3,n∈ $Z^2$ is a tight frame for $L_2(R^2)$ In both cases, the frame bounds are equal to1. Since *Wj* is generated by four kernel functions (similar to multi-wavelets), in general it is not a shift-invariant subspace. Nevertheless, a shift-invariant subspace can be simulated by denoting:

$$\mu_{j,2n+k_i}(t) = \Psi_{j,n}^{(i)}(t), 0 \le i \le 3 \quad (7)$$

where ki are the coset representatives for down sampling by 2 in each dimension, i.e.,

k0=(0,0)T, k1=(1,0)T, k2=(0,1)T, k3=(1,1) (8)

With this notation, the family $\{\mu_{j,n}\}, n \in Z^2$ associated to a uniform grid of intervals $2^{j-1}$x $2^{j-1}$ on $R^2$ provides a tight frame for $W_j$.

**3.2.3 Multidirection Analysis**

Using multirate identities [12], it is instructive to view an l-level tree-structured DFB equivalently as a $2^1$ parallel channel filter bank, as in Fig.(2.a), with equivalent analysis filters, synthesis filters and overall sampling matrices. The equivalent directional analysis filters are denoted as $E_k^{(l)}, 0 \le k \le 2^l$ and the directional synthesis filters as $D_k^{(l)}, 0 \le k < 2^l$, which corresponds to the subbands.

The corresponding overall sampling matrices $S_k^l$ are proved to have the following diagonal forms [12].

$$S_k^l = \begin{cases} \begin{bmatrix} 2^{l-1} & 0 \\ 0 & 2 \end{bmatrix} \\ \begin{bmatrix} 2 & 0 \\ 0 & 2^{l-1} \end{bmatrix} \end{cases} \quad (9)$$

which means sampling is separable. The two sets correspond to the mostly horizontal and mostly vertical set of directions, respectively. From the equivalent parallel view of the DFB, it can be seen that the family

$$\left\{ d_k^{(l)}\left[n - S_k^{(l)} m\right] \right\} \; 0 \le k < 2^l, m \in Z^2 \quad (10)$$

obtained by translating the impulse responses of the equivalent synthesis filters $D_k^{(l)}$ over the sampling lattices by $S_k^{(l)}$ , provides a basis for discrete signals in L2(z2).

This basis exhibits both directional and localization properties. In the iterated contourlet filter bank, the discrete basis (9) of the DFB can be regarded as a change of basis for the continuous-domain subspaces from the multiscale analysis of the previous LP stage. Suppose that the DFB in the contourlet filter bank utilizes orthogonal filters and when such DFB is applied to the difference image (detail) subspaces then the resulting detail directional subspaces $W_{j,k}^{(l)}$ in the frequency domain will be as illustrated in Fig.(2.b)

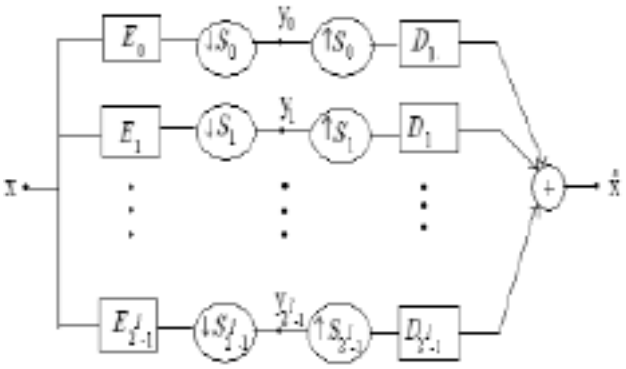

**Fig 3(a) Multichannel view of a l-level tree structured DFB**

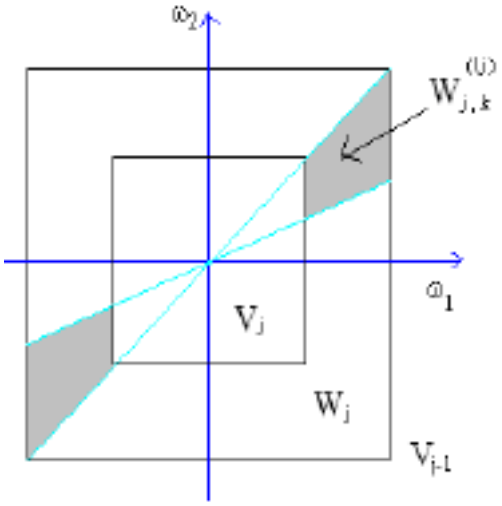


**Fig 3(b) Multiscale and multidirection subspaces**

Thus, the contourlet is applied over the blocks of an image and then the features of each block are extracted and are explained in the forthcoming section.

## 3. Feature Extraction

Feature extraction is a type of dimensionality reduction from which the region of interest can alone be extracted. In this work, features such as Gray level non-uniformity, Run length non-uniformity, run percentage and long run emphasis are extracted from the image blocks.

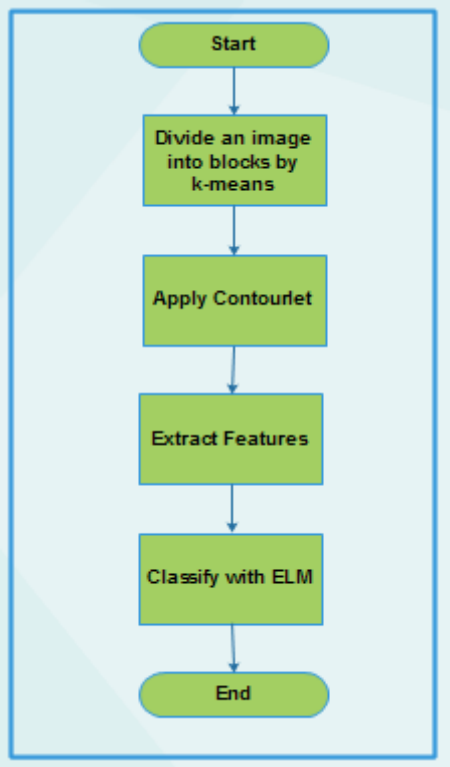


**Fig 4: Overall flow of the System**

### 3.1 Gray Level Non-uniformity (GLN)

GLN measures the similarity of gray level values throughout the image. The GLN value will be small if the gray level values resemble the same throughout the image and is given by eqn 11.

$$RL_{gln} = \frac{1}{n_r}\sum_{i=1}^{M}\left(\sum_{j=1}^{N} p[i,j]\right)^2 \quad (11)$$

### 3.2 Run Length Non-uniformity (RLN)

RLN measures the similarity of the length of runs throughout the image. RLN is smaller if the run lengths are alike throughout the image.

$$RL_{rln} = \frac{1}{n_r}\sum_{j=1}^{N}\left(\sum_{i=1}^{M} p[i,j]\right)^2 \quad (12)$$

### 3.3 Run Percentage (RPC)

Run Percentage measures the homogeneity and the distribution of runs in an image along a specific direction. RPC is the largest when the length of runs is 1 for all gray levels in specific direction.

$$RL_{rpc} = \frac{n_r}{p[i,j]*j} \quad (13)$$

### 3.4 Long Run Emphasis (LRE)

LRE measures the distribution of long runs and is dependent on the occurrence of long runs and is expected large for coarse structural textures and is presented below.

$$RL_{02} = \frac{1}{n_r}\sum_{i=1}^{M}\sum_{j=1}^{N} p[i,j] * j^2 \quad (14)$$

All the above mentioned features are extracted from the blocks of an image. The classifier is then applied to the image, in order to determine the nature of an image.

## 4. ELM classification

ELM is the fastest learning classifier. The ELM is trained with the extracted features and when an image is tested for its nature, ELM determines whether or not the image is stego. A standard single layer feed forward neural network with n number of neurons and it can given by

$$\sum_i Wn_i g\left(Win_i x_j + th_i\right) = k_j \quad (15)$$

Where $Win_i$ is the weight vector connecting inputs, i is the hidden neurons, $Wn_i$ is the weight vector connecting hidden neurons, $th_i$ is the threshold of the $i^{th}$ hidden neuron. $k_j$ is the output of ELM.

**Algorithm**

Input: Training set, activation function g(x), number of hidden neurons n, input weight $W_i$

Step 1: The hidden layer output matrix is detected M.

Step 2: The output weight is calculated by

$$\widetilde{Wn} = M'T \quad (16)$$

Where $M'$ is the Moore-Penrose generalized inverse of M. The trained ELM can effectively classify between the stego and the normal image. The performance of the proposed work is proved by the experimental results.

## 4. Performance Analysis

The performance of this work is analyzed by comparing with several existing methodologies. The proposed work is compared with LSB steganalysis, Neural network based steganalysis, DWT steganalysis and JPEG steganalysis. The performance metrics employed for comparison are true positive, true negative, false positive, false negative, accuracy, specificity and sensitivity.

### 4.1 True Positive (TP)

True Positive (TP) is the proportion of positive cases that were correctly identified, as calculated using the equation.

$$TP = \frac{Number\ of\ Correctly\ classified\ images}{Total\ number\ of\ images} \times 100 \quad (17)$$

### 4.2 True Negative (TN)

True Negative (TN) is defined as the proportion of negatives cases that were classified correctly, as calculated using the equation.

$$TN = \frac{Number\ of\ falsely\ classified\ images}{Total\ number\ of\ images} \times 100 \quad (18)$$

### 4.3 False Positive (FP)

False Positive (FP) is the proportion of negatives cases that were incorrectly classified as positive, as calculated using the equation.

$$FP = \frac{Number\ of\ correctly\ classified\ images}{Total\ number\ of\ images} \times 100 \quad (19)$$

### 4.4 False Negative (FN)

False Negative (FN) is the proportion of positives cases that were incorrectly classified as negative, as calculated using the equation.

$$FN = \frac{Number\ of\ falsely\ classified\ images}{Total\ number\ of\ images} \times 100 \quad (20)$$

With the above mentioned parameters, the accuracy, sensitivity and specificity are calculated and the results are shown in graphs. From the experimental results, it is evident that the proposed system works well than the others.

### 4.5 Accuracy Value

The accuracy of a measurement system is the degree of closeness of measurements of a quantity to that quantity's actual (true) value.

$$Accuracy = \frac{TP+TN}{TP+TN+FP+FN} \quad (21)$$

### 4.6 Specificity Value

Specificity measures the proportion of negatives which are correctly identified such as the percentage of healthy people who are correctly identified as not having the condition, sometimes called the true negative rate.

$$S_p = \frac{TN}{TN+FP} \quad (22)$$

### 4.7 Sensitivity Value

Sensitivity also called the true positive rate or the recall rate in some field's measures the proportion of actual positives which are correctly identified.

$$S_e = \frac{TP}{TP+FN} \tag{23}$$

**Table 1: Performance Analysis**

| Techniques | TP | TN | FP | FN | Accuracy | Sensitivity | Specificity |
|---|---|---|---|---|---|---|---|
| Proposed Work | 94 | 10 | 5 | 3 | 0.928571 | 0.969072 | 0.666667 |
| LSB Steganalysis | 87 | 25 | 12 | 9 | 0.842105 | 0.90625 | 0.675676 |
| Neural Network based Steganalysis | 75 | 26 | 19 | 10 | 0.776923 | 0.882353 | 0.577778 |
| DWT Steganalysis | 71 | 29 | 22 | 15 | 0.729927 | 0.825581 | 0.568627 |
| JPEG Steganalysis | 68 | 30 | 24 | 17 | 0.705036 | 0.8 | 0.555556 |

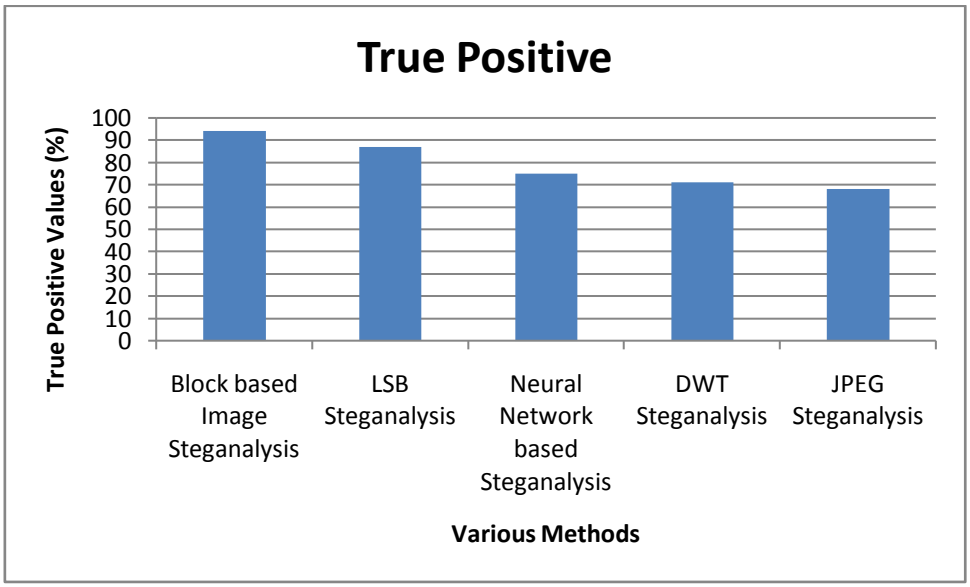


**Fig 5: True Positive Analysis**

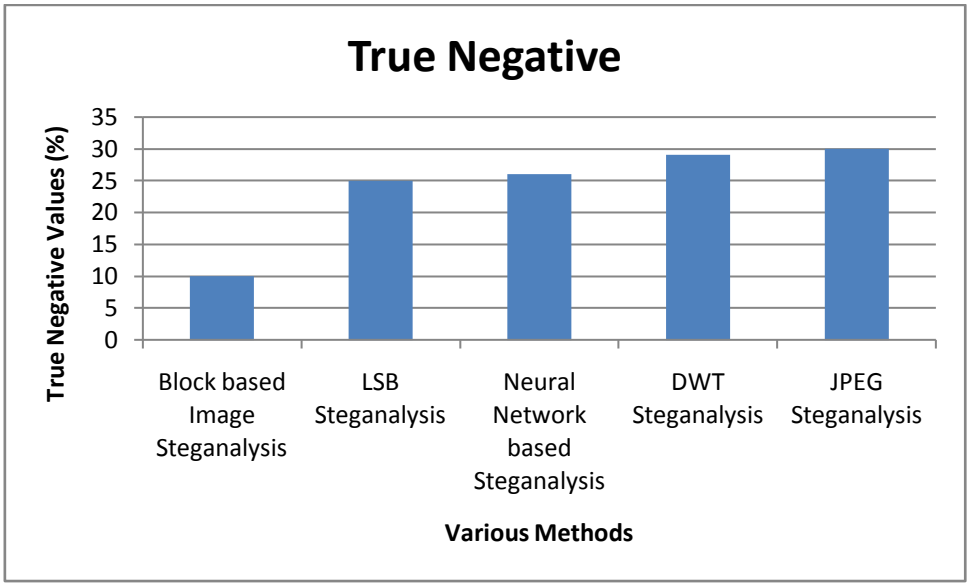


**Fig 6: True Positive Analysis**

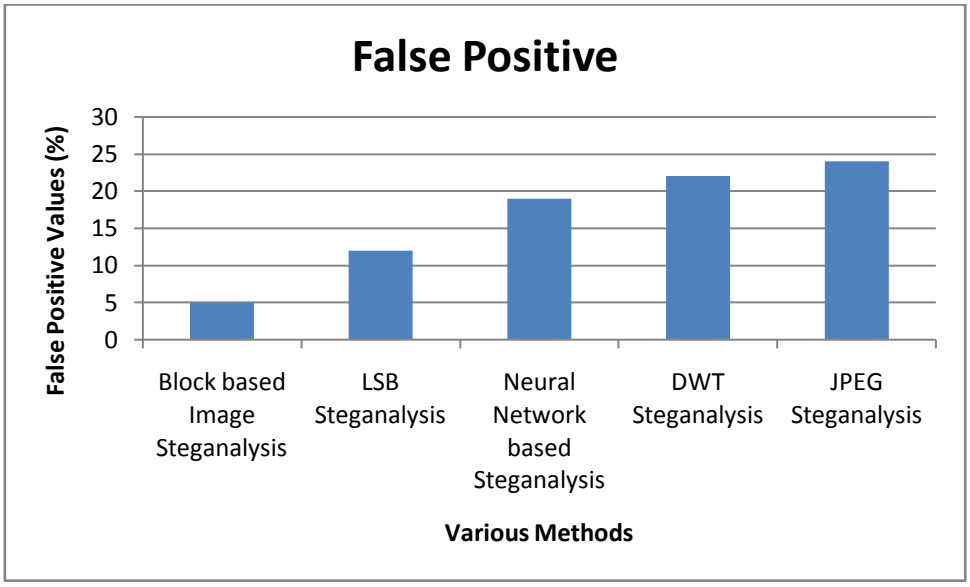


**Fig 7: False Positive Analysis**

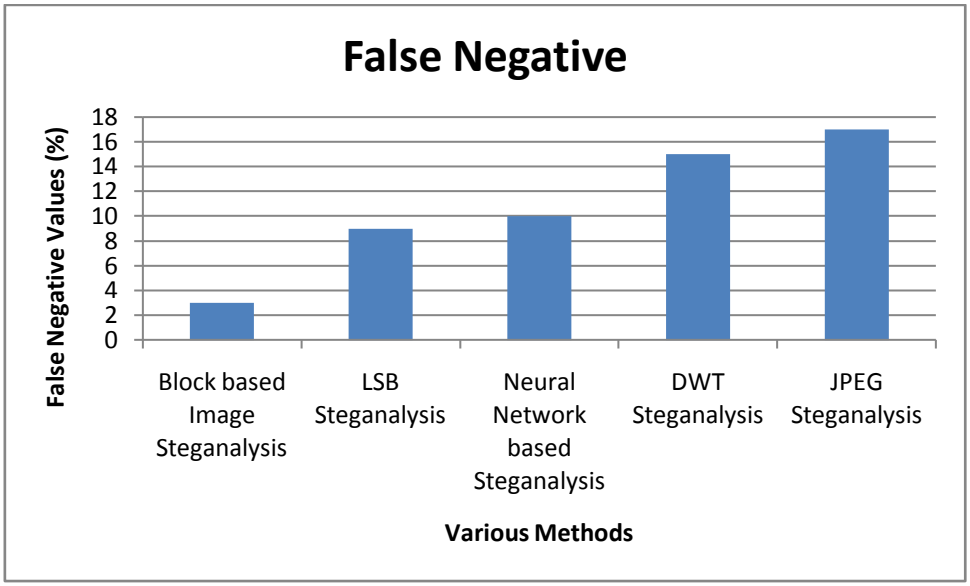


**Fig 8: False Negative Analysis**

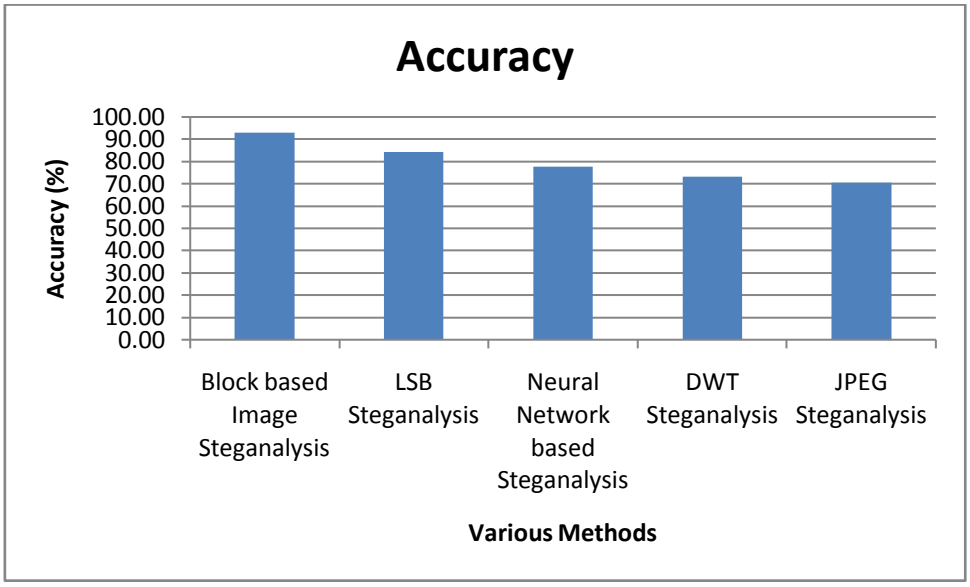


**Fig 9: Accuracy Analysis**

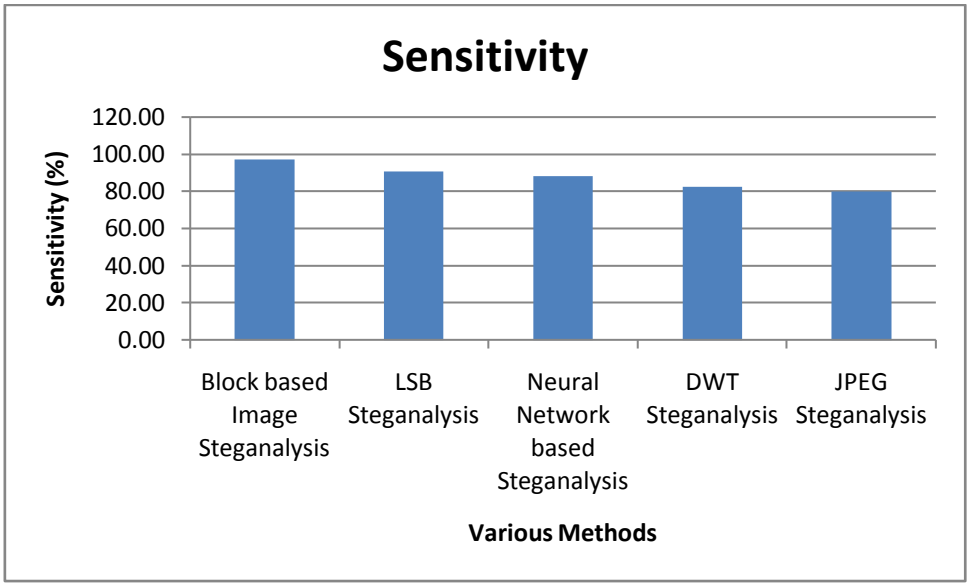


**Fig 10: Sensitivity Analysis**

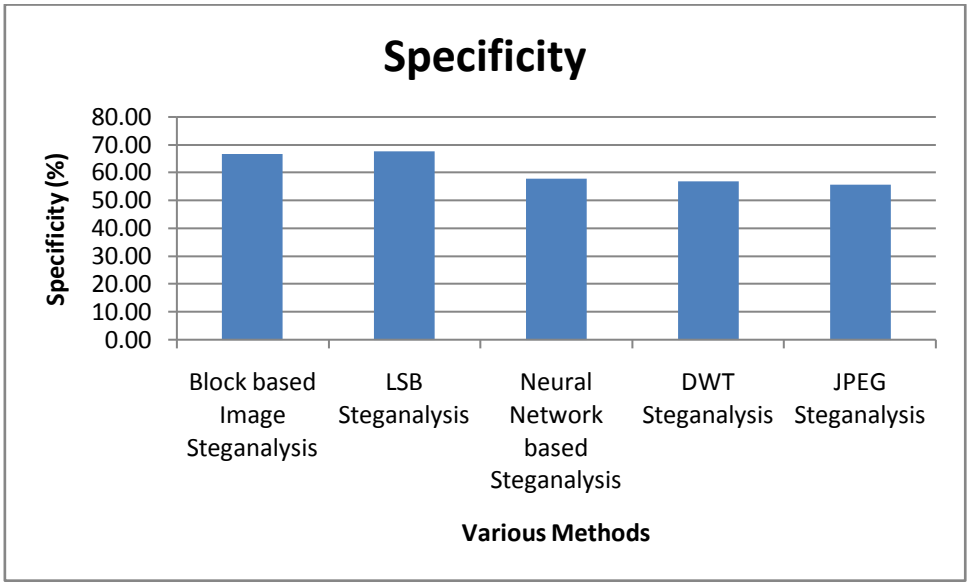


**Fig 11: Specificity Analysis**

Thus, from the experimental results, it is evident that the proposed work outperforms several steganalysis techniques. The accuracy rate of proposed work is 92.8% and the sensitivity rate is 96.9%.

## Conclusion

In this work, a steganalysis technique is proposed with four different phases. In the

first phase, the image is decomposed into several blocks. This is followed by the application of contourlet and then the features are extracted from the image. ELM is trained with these features and tested with another set of images. This work proves 92.8% accuracy and 96.9% sensitivity rate.

## References

[1] Abbas Cheddad, Joan Condell, Kevin Curran and Paul Mc Kevitt, "Digital Image Steganography: Survey and analysis of current methods", Signal Processing, March 2010, Pages 727-752.

[2] Ismail Avcibas, Mehdi Kharrazi, Nasir Memon, Bulent Sankur, "Image Steganalysis with Binary Similarity Measure-s", EURASIP Journal on Applied Signal Processing, January 2005, Pages 2749 - 2757.

[3] ] J. Fridrich, "Feature-based steganalysis for JPEG images and its implications for future design of steganographic schemes," in 6th Information Hiding Workshop, Toronto, ON, Canada, 2004.

[4] C. Chen and Y. Q. Shi, "JPEG image steganalysis utilizing both intrablock and interblock correlations," in IEEE ISCAS, International Symposium on Circuits and Systems, Seattle, Washington, USA, 2008.

[5] J. Fridrich and T. Pevny, "Merging Markov and DCT features for multiclass JPEG steganalysis," in Proc. SPIE Electronic Imaging,Security, Steganography, and Watermarking of Multimedia Contents IX, San Jose, CA, 2007.

[6] T. Pevný, P. Bas and J. Fridrich, "Steganalysis by Subtractive Pixel Adjacency Matrix," IEEE Transactions on Information Forensics and Security, vol. 5, no. 2, pp. 215-224, June 2010.

[7] Q. Liu, A. H. Sung and M. Qiao, "Improved Detection and Evaluation for JPEG Steganalysis," in 17th ACM international conference on Multimedia, Beijing, China, 2009.

[8] D. Zou, Y. Q. Shi, W. Su and G. Xuan, "Steganalysis Based On Markov Model Of Thresholded Prediction-Error Image," in IEEE International Conference on Multimedia and Expo, Toronto, Ontario, Canada, 2006.

[9] M. Seyedhosseini and S. Ghaemmaghami, "Detection of LSB Replacement and LSB Matching Steganography Using Gray Level Run Length Matrix," in Fifth International Conference on Intelligent Information Hiding and Multimedia Signal Processing, Kyoto, Japan, 2009.

[10] T. J. Benedict Jose, P. Eswaran, "Effective Steganalytic Algorithm based on Residual Value of Pixels in an Image", International Journal of Advanced Computer Research, Vol.3, pp. 32-36, 2013.

[11] T. J. Benedict Jose, P. Eswaran, "An Efficient Steganalytic Algorithm based on Contourlet with GLCM", Accepted for publication, Research Journal of Applied Sciences, Engineering and Technology, 2013.

[12] W. Zhu, Z. Xiong, and Y.-Q. Zhang, "Multiresolution watermarking for images and video: A unified approach," in Proc. ICIP98, Chicago, IL, Oct. 1998.

[13] Dr.Jassim, et al, "Digital Photography and Imaging", Alameda, California, USA, SYPEX Inc. 272 p., 2010.

[14] Veenu Bhasin,Punam Bedi, "Steganalysis of Colored JPEG Images using Ensemble of Extreme Learning Machines ", Int. J. on Recent Trends in Engineering and Technology, Vol. 11, pp.63-74, 2014.